

**FIELD PERFORMANCE OF FLEXIBLE PAVEMENT
CONSTRUCTED WITH COPPER AND STEEL
INDUSTRY WASTES IN SUBBASE LAYER**

MAYURESH DHANRAJ BAKARE



**DEPARTMENT OF CIVIL ENGINEERING
INDIAN INSTITUTE OF TECHNOLOGY DELHI
FEBRUARY 2024**

© Indian Institute of Technology Delhi (IITD), New Delhi, 2024

**FIELD PERFORMANCE OF FLEXIBLE PAVEMENT
CONSTRUCTED WITH COPPER AND STEEL
INDUSTRY WASTES IN SUBBASE LAYER**

by

MAYURESH DHANRAJ BAKARE

DEPARTMENT OF CIVIL ENGINEERING

submitted

in fulfilment of the requirements of the degree of doctor of philosophy

to the



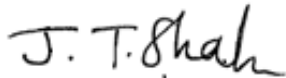
INDIAN INSTITUTE OF TECHNOLOGY DELHI

FEBRUARY 2024

Dedicated to
my
Parents

CERTIFICATE

This is to certify that the thesis titled “**Field Performance of Flexible Pavement Constructed with Copper and Steel Industry Wastes in Subbase Layer**”, submitted by **Mr. Mayuresh D. Bakare** to the Indian Institute of Technology Delhi is a record of bonafide research work carried out by him under our supervision and guidance. This thesis work, in our opinion, has reached the standard of fulfilling the requirements for a **Doctor of Philosophy** degree. The research report and results presented in this thesis have not been submitted, in part or full, to any University or Institute for the award of the degree or diploma.



Dr. J. T. Shah

Professor,
Department of Civil Engineering,
IIT Delhi
New Delhi - 110016



Dr. Satyajit. Patel

Associate Professor
Department of Civil Engineering,
SVNIT Surat
Surat - 395007

ACKNOWLEDGEMENTS

I am profoundly grateful and indebted to my distinguished supervisor, Prof. J. T. Shahu, for his invaluable guidance, unwavering belief in my abilities, and steadfast support. In the same breath, I extend my heartfelt gratitude to my co-supervisor, Prof. Satyajit Patel of SVNIT Surat, for his pivotal role in planning and executing the construction, as well as his unfaltering backing during the demanding fieldwork. Throughout our enduring collaboration, both have expertly nurtured the development of my ideas and the deepening of my understanding. Without their dedicated supervision, constant encouragement, and wholehearted support, this thesis and the subsequent publications stemming from our work would not have materialized. I am immensely thankful to both for their faith in me and for allowing me to explore innovative concepts within the framework of a well-funded field project.

I sincerely appreciate the Student Research Committee members, namely Prof. D.R. Kaushal, Prof. A. K. Swamy, and Prof. S. Pradyumna, for their invaluable suggestions during this work. I am humbled by the unwavering support of the esteemed faculty members from the civil engineering departments of both IIT Delhi and SVNIT Surat, whose constant encouragement was instrumental in this endeavor. I must also acknowledge the indispensable assistance provided by the laboratory technicians at both these institutes.

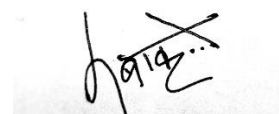
I would like to express my gratitude to the Department of Science and Technology, Government of India for their generous financial support, which enabled the successful completion of this work. Additionally, I extend my appreciation to the Road and Building Department, Surat, and the Surat Municipal Corporation for their support during fieldwork, with special thanks to Chief Engineer P. M. Chaudhari and Assistant Engineer Kalpesh Thorat for their invaluable assistance during construction and field testing.

I am deeply grateful to Dr. Rahul Pai, Dr. Rohan Deshmukh, Mr. Sandeep Singh, Dr. Hrishikesh Shahane from SVNIT Surat, who assisted me during the field testing, and Dr. Abhishek Srivastava, Dr. Rahul Singh, Mr. Deepesh Bansal, and Mr. Devprakash Parida for their support in conducting leaching tests at IIT Delhi.

My journey was made more manageable by the unwavering support of a circle of supportive seniors and friends, including but not limited to Mrs. Sujata Fulambarkar, Mr. Lalit Kandpal, Dr. Pranjal Mandhaniya, Dr. Riya Bhaumik, Dr. Prasun Halder, Dr. Apoorva Agrawal, Mr. Aniket Shirgaonkar, Dr. Shubham Kalore, Mr. Vinay Singh and Ms. Shweta Lokhande. Their spiritual and moral support transformed this challenging task into a pleasurable experience. I also sincerely thank my old friends, colleagues, and well-wishers for their valuable suggestions and assistance in completing this project. To those whose names are not mentioned here, your direct or indirect support is equally appreciated.

I want to express my deepest gratitude to my parents, Adv. Dhanraj Balaji Bakare and Adv. Vidya Dhanraj Bakare, who provided spiritual and moral support, love, and understanding. Without their many sacrifices, my dream of completing a PhD would have remained unfulfilled.

If anyone's explicit mention is inadvertently omitted, it is due more to the limitations of my memory than any lack of appreciation. I apologize for any oversights. Finally, I express my gratitude to the Almighty for blessing me with health and strength, without which none of this would have been possible.



Mayuresh D. Bakare

ABSTRACT

To sustainably counter the problems of depleting natural aggregate resources and environmentally injurious metal slag and flyash open dumps, establishing the technical and economic feasibility of using industrial wastes to replace the natural aggregate is the need of the hour. In this regard, Dr. Satyajit Patel, in his doctoral thesis (Patel 2016), proposed three innovative industrial waste mixes for their use to completely replace the granular subbase (GSB) in a typical flexible pavement. However, for the construction industry to adopt laboratory-based technology, it is imperative to evaluate the performance of the above mixes in a field pilot study. Therefore, this dissertation focused on the techno-economic feasibility of the complete substitution of granular subbase with the three industrial waste mixes as given below, in a typical four-layered flexible pavement based on a medium-term (3 years 9 months) prototype field performance.

1. FAL - Flyash + 5% lime
2. CFA - 70% Copper Slag + 30% Flyash and
3. FAG - 80% Flyash + 20% Granulated blast furnace slag

First, these proportions of optimum waste mixes were reassessed by performing laboratory tests such as Unconfined Compressive Strength (UCS) test, California Bearing Ratio (CBR) triaxial shear strength test and cyclic triaxial test (CTT) because compared to Patel (2016), the flyash had higher lime content and dolime was replaced by lime as the activator. These differences resulted in higher strengths and stiffnesses in CFA and FAG and lower optimum activator dose in FAL compared to Patel (2016).

Using the laboratory test results, ten flexible pavement test sections, each 50 m long and 3.5 m wide, were designed and constructed as a part of State Highway No. 6 near Surat, Gujarat. Nine sections had FAL, CFA and FAG subbase layers in three varying thicknesses (200 mm,

300 mm and 400 mm), and the tenth section, the control section, had a granular subbase (GSB) of 330 mm thickness as a baseline case for comparison. The structural and functional performance of the test sections was evaluated in four phases using Falling Weight Deflectometer (FWD) and Bump Integrator (BI). Initially, FWD tests were conducted monthly to study the effect of curing. Once the peak E_{FWD} (backcalculated FWD moduli) of the subbase layers were recorded after nine months, a coring operation was conducted to compare the strength gain in the field and laboratory using microstructure analysis. Secondly, post-peak performance, FWD and BI tests were performed pre- and post-monsoon to study the effect of seasonal moisture variation and related structural and functional changes and damages in the test sections. In the third phase, after two years, a truck overloading operation was conducted post-monsoon to simulate seasonal overloading during harvesting and the associated damage sustained by the test sections. During the third and fourth years, post-damage performance typical to pavements with waste mix subbase layers was captured in the final phase. Heavy metal leaching potential was assessed by conducting TCLP and water leaching tests on the raw wastes and field core samples and by testing the leachate collected from the drains installed in the test sections.

Additionally, the nonlinear behaviour of E_{FWD} of FAL, CFA and FAG subbases in field and laboratory was compared by deriving stress-dependent conversion factors based on two constitutive models to convert M_r to E_{FWD} at different field testing phases. Finally, LCA and construction and maintenance cost analyses were conducted to attest to the environmental and economic feasibility of using the waste mixes as subbase layers in typical Indian flexible pavement state highways.

The waste mix subbase took three months to reach stable moduli values that were 3 to 5 times higher than GSB. Due to less variation in the subbase modulus owing to changes in moisture content and inherent higher stiffness, waste mix subbase layers sustained an extreme

condition of post-monsoon truck overloading without premature failure. No significant surface distress was found in waste mix test sections in terms of rutting, cracking, or heaving, substantiating the robustness of the waste mix subbase layers. The failure mechanism of the waste mix test sections showed that the damage begins with stabilized waste mix layers and propagates upwards. The waste mixes produced stable pozzolanic binding gels, immobilizing the heavy metals in the raw wastes with no signs of heaving. Thus, the waste mix subbase does not possess any potential to contaminate the ground water with heavy metals. Stabilized waste mixes exhibited stress hardening with increasing bulk and deviatoric stresses in the field and laboratory. Curing increases E_{FWD} and reduces its sensitivity to stress. In contrast, traffic damage imparts the opposite effect as the stabilized waste mixes transform into cracked and blocky mass. This information would allow practitioners to predict the field performance of the waste mix subbase with great accuracy, resulting in a reliable design and possible cost savings.

As per remaining fatigue life, a 330 mm thick GSB in a flexible pavement can be replaced with even a 200 mm thick FAL, FAG or CFA layers with 30% – 100% higher fatigue design life, 13% – 23% lower surface roughness after 3 years and 9 months. This higher fatigue life resulted in lower overlay thicknesses at the end of the test period. This resulted in 12.5% to 30% lower overall costs. Due to avoided burdens of quarrying and processing stones to produce natural aggregates, savings in valuable land occupied by dumpsites and shorter transport distance from the raw material sources to construction, all the alternatives to GSB were sustainable with 45 % to 65% lower relative life cycle environmental impacts compared to the control section. This knowledge can be used to minimize thicknesses of different layers, such as HMA and base layers, and achieve a more economical design for construction.

सार

घटते प्राकृतिक समुच्चय संसाधनों और पर्यावरण के लिए हानिकारक धातु स्लैग और फ्लाईएश के खुले डंप की समस्याओं का स्थायी रूप से मुकाबला करने के लिए, प्राकृतिक समुच्चय को बदलने के लिए औद्योगिक कचरे का उपयोग करने की तकनीकी और आर्थिक व्यवहार्यता स्थापित करना समय की मांग है। इस संबंध में, डॉ. सत्यजीत पटेल ने अपने डॉक्टरेट थीसिस (पटेल 2016) में, एक विशिष्ट लचीले फुटपाथ में ग्रैनुलर सबबेस (जीएसबी) को पूरी तरह से बदलने के लिए उनके उपयोग के लिए तीन अभिनव औद्योगिक अपशिष्ट मिश्रणों का प्रस्ताव रखा। हालाँकि, निर्माण उद्योग के लिए प्रयोगशाला-आधारित प्रौद्योगिकी को अपनाने के लिए, फ्रील्ड पायलट अध्ययन में उपरोक्त मिश्रणों के प्रदर्शन का मूल्यांकन करना अनिवार्य है। इसलिए, यह शोध प्रबंध एक मध्यम अवधि (3 वर्ष 9 महीने) प्रोटोटाइप क्षेत्र के आधार पर एक विशिष्ट चार-परत लचीले फुटपाथ में नीचे दिए गए तीन औद्योगिक अपशिष्ट मिश्रणों के साथ दानेदार उप-आधार के पूर्ण प्रतिस्थापन की तकनीकी-आर्थिक व्यवहार्यता पर केंद्रित है। प्रदर्शन।

4. एफएएल - फ्लाईएश + 5% चूना
5. सीएफए - 70% कॉपर स्लैग + 30% फ्लाईएश और
6. एफएजी - 80% फ्लाईएश + 20% दानेदार ब्लास्ट फर्नेस स्लैग

सबसे पहले, इष्टतम अपशिष्ट मिश्रणों के इन अनुपातों का प्रयोगशाला परीक्षणों जैसे कि अपुष्ट संपीड़न शक्ति (यूसीएस) परीक्षण, कैलिफ़ोर्निया बियरिंग अनुपात (सीबीआर) त्रिअक्षीय कतरनी शक्ति परीक्षण और चक्रीय त्रिअक्षीय परीक्षण (सीटीटी) द्वारा पुनः मूल्यांकन किया गया क्योंकि पटेल (2016) की तुलना में, फ्लाईएश में चूने की मात्रा अधिक थी और एक्टिवेटर के रूप में डोलाइम को चूने से बदल दिया गया था। इन अंतरों के परिणामस्वरूप पटेल (2016) की तुलना में सीएफए और एफएजी में उच्च ताकत और कठोरता और एफएएल में कम इष्टतम एक्टिवेटर खुराक हुई।

प्रयोगशाला परीक्षण परिणामों का उपयोग करते हुए, दस लचीले फुटपाथ परीक्षण खंड, प्रत्येक 50 मीटर लंबे और 3.5 मीटर चौड़े, सूरत, गुजरात के पास राज्य राजमार्ग संख्या 6 के एक हिस्से के रूप में डिजाइन और

निर्मित किए गए थे। नौ खंडों में तीन अलग-अलग मोटाई (200 मिमी, 300 मिमी और 400 मिमी) में एफएएल, सीएफए और एफएजी सबबेस परतें थीं, और दसवें खंड, नियंत्रण खंड में बेसलाइन केस के रूप में 330 मिमी मोटाई का एक दानेदार सबबेस (जीएसबी) था। तुलना। परीक्षण अनुभागों के संरचनात्मक और कार्यात्मक प्रदर्शन का मूल्यांकन फॉलिंग वेट डिफ्लेक्टोमीटर (एफडब्ल्यूडी) और बम्प इंटीग्रेटर (बीआई) का उपयोग करके चार चरणों में किया गया था। प्रारंभ में, इलाज के प्रभाव का अध्ययन करने के लिए एफडब्ल्यूडी परीक्षण मासिक रूप से आयोजित किए गए थे। एक बार जब नौ महीने के बाद सबबेस परतों का शिखर ई^{एफडब्ल्यूडी} (बैककैलकुलेटेड एफडब्ल्यूडी मॉड्यूल) दर्ज किया गया, तो माइक्रोस्ट्रक्चर विश्लेषण का उपयोग करके क्षेत्र और प्रयोगशाला में ताकत लाभ की तुलना करने के लिए एक कोरिंग ऑपरेशन आयोजित किया गया था। दूसरे, परीक्षण खंडों में मौसमी नमी भिन्नता और संबंधित संरचनात्मक और कार्यात्मक परिवर्तनों और क्षति के प्रभाव का अध्ययन करने के लिए पोस्ट-पीक प्रदर्शन, एफडब्ल्यूडी और बीआई परीक्षण मानसून से पहले और बाद में आयोजित किए गए थे। तीसरे चरण में, दो वर्षों के बाद, कटाई के दौरान मौसमी ओवरलोडिंग और परीक्षण अनुभागों को होने वाले संबंधित नुकसान का अनुकरण करने के लिए मानसून के बाद एक ट्रक ओवरलोडिंग ऑपरेशन चलाया गया। तीसरे और चौथे वर्ष के दौरान, अपशिष्ट मिश्रण सबबेस परतों के साथ फुटपाथों के लिए विशिष्ट क्षति के बाद के प्रदर्शन को अंतिम चरण में कैप्चर किया गया था। भारी धातु लीचिंग क्षमता का आकलन कच्चे अपशिष्टों और फील्ड कोर नमूनों पर टीसीएलपी और जल लीचिंग परीक्षण करके और परीक्षण खंडों में स्थापित नालियों से एकत्रित लीचेट का परीक्षण करके किया गया था।

एफएएल, सीएफए और एफएजी सबबेस के ई^{एफडब्ल्यूडी} के गैर-रेखीय व्यवहार की तुलना विभिन्न क्षेत्र परीक्षण चरणों में एम^{आर} को ई^{एफडब्ल्यूडी} में परिवर्तित करने के लिए दो संवैधानिक मॉडल के आधार पर तनाव-निर्भर रूपांतरण कारकों को प्राप्त करके की गई थी। अंत में, विशिष्ट भारतीय लचीले फुटपाथ राज्य राजमार्गों में उप-आधार परतों के रूप में अपशिष्ट मिश्रण का उपयोग करने की पर्यावरणीय और आर्थिक व्यवहार्यता को प्रमाणित करने के लिए एलसीए और निर्माण और रखरखाव लागत विश्लेषण आयोजित किए गए।

अपशिष्ट मिश्रण सबबेस को स्थिर मॉड्यूल मान तक पहुंचने में तीन महीने लगे जो जीएसबी से 3 से 5 गुना अधिक थे। नमी की मात्रा में परिवर्तन और अंतर्निहित उच्च कठोरता के कारण सबबेस मापांक में कम भिन्नता के कारण, अपशिष्ट मिश्रण सबबेस परतों ने समय से पहले विफलता के बिना मानसून के बाद ट्रक ओवरलोडिंग की

चरम स्थिति को बनाए रखा। अपशिष्ट मिश्रण परीक्षण अनुभागों में सड़न, दरार या भारीपन के संदर्भ में कोई महत्वपूर्ण सतह संकट नहीं पाया गया , जो अपशिष्ट मिश्रण सबबेस परतों की मजबूती को प्रमाणित करता है। अपशिष्ट मिश्रण परीक्षण अनुभागों की विफलता तंत्र से पता चला कि क्षति स्थिर अपशिष्ट मिश्रण परतों से शुरू होती है और ऊपर की ओर बढ़ती है। अपशिष्ट मिश्रण से स्थिर पॉज़ोलानिक बाइंडिंग जैल का उत्पादन होता है, जो कच्चे कचरे में भारी धातुओं को स्थिर कर देता है, जिसमें भारीपन का कोई संकेत नहीं होता है। इस प्रकार, अपशिष्ट मिश्रण उपआधार में भारी धातुओं के साथ भूजल को दूषित करने की कोई क्षमता नहीं होती है। स्थिर अपशिष्ट मिश्रणों ने क्षेत्र और प्रयोगशाला में बढ़ते थोक और विचलन तनाव के साथ तनाव सख्त होने का प्रदर्शन किया। इलाज से ई ^{एफ.डब्ल्यू.डी} बढ़ता है और तनाव के प्रति इसकी संवेदनशीलता कम हो जाती है। इसके विपरीत, यातायात क्षति विपरीत प्रभाव डालती है क्योंकि स्थिर अपशिष्ट मिश्रण फटे और अवरुद्ध द्रव्यमान में बदल जाता है। यह जानकारी चिकित्सकों को बड़ी सटीकता के साथ अपशिष्ट मिश्रण उप-आधार के क्षेत्र प्रदर्शन की भविष्यवाणी करने की अनुमति देगी, जिसके परिणामस्वरूप एक विश्वसनीय डिजाइन और संभावित लागत बचत होगी।

शेष थकान जीवन के अनुसार, लचीले फुटपाथ में 330 मिमी मोटी जीएसबी को 200 मिमी मोटी एफएएल, एफएजी या सीएफए परतों के साथ 30% - 100% अधिक थकान डिजाइन जीवन, 13% - 23% कम सतह खुरदरापन के साथ बदला जा सकता है। 3 साल और 9 महीने. इस उच्च थकान जीवन के परिणामस्वरूप परीक्षण अवधि के अंत में ओवरले की मोटाई कम हो गई। इसके परिणामस्वरूप कुल लागत 12.5% से 30% कम हो गई। प्राकृतिक समुच्चय का उत्पादन करने के लिए पत्थरों के उत्खनन और प्रसंस्करण के बोझ से बचने, डंपसाइटों द्वारा कब्जा की गई मूल्यवान भूमि में बचत और कच्चे माल के स्रोतों से निर्माण तक कम परिवहन दूरी के कारण, जीएसबी के सभी विकल्प 45% से 65% कम सापेक्ष जीवन चक्र के साथ टिकाऊ थे। नियंत्रण अनुभाग की तुलना में पर्यावरणीय प्रभाव। इस ज्ञान का उपयोग विभिन्न परतों, जैसे एचएमए और आधार परतों की मोटाई को कम करने और निर्माण के लिए अधिक किफायती डिजाइन प्राप्त करने के लिए किया जा सकता है।

TABLE OF CONTENTS

CERTIFICATE	I
ACKNOWLEDGEMENTS	II
ABSTRACT	IV
संर	VII
TABLE OF CONTENTS	X
LIST OF FIGURES	XVI
LIST OF TABLES	XXI
LIST OF ABBREVIATIONS	XXIV
LIST OF NOTATIONS	XXVIII
CHAPTER 1 INTRODUCTION	1
1.1 BACKGROUND.....	1
1.2 NEED FOR THE STUDY.....	3
1.3 OBJECTIVES AND SCOPE OF THE STUDY.....	4
1.4 METHODOLOGY.....	6
1.5 ORGANIZATION OF THE THESIS.....	9
CHAPTER 2 LITERATURE REVIEW	12
2.1 INTRODUCTION.....	12
2.2 SLAG GENERATION IN COPPER AND STEEL INDUSTRIES.....	12
2.2.1 <i>Copper Slag</i>	12
2.2.2 <i>Blast Furnace Slag</i>	15

2.3	USE OF INDUSTRIAL WASTE IN PAVEMENT LAYERS	17
2.4	FWD FOR STRUCTURAL EVALUATION OF PAVEMENT	18
2.4.1	<i>FWD working principles</i>	18
2.4.2	<i>Backcalculation of Field Modulus</i>	19
2.4.3	<i>Field Studies</i>	20
2.4.4	<i>Comparison between Field and Laboratory Moduli</i>	31
2.4.5	<i>Seasonal variation in pavement performance</i>	35
2.4.6	<i>Application of Deflection Basin Parameters</i>	39
2.5	USE OF LWD AND DCPT IN QA/QC WORKS	44
2.6	MEASUREMENT OF ROUGHNESS OF FLEXIBLE PAVEMENT	45
2.7	FORENSIC GEOTECH INVESTIGATION OF PAVEMENT DAMAGE	46
2.8	LIFE CYCLE ASSESSMENT	48
2.9	RESEARCH GAPS	51
CHAPTER 3 MATERIALS AND LABORATORY STUDIES		54
3.1	INTRODUCTION	54
3.2	RAW MATERIALS AND TRIAL WASTE MIX PROPORTIONS	55
3.2.1	<i>Physical and Chemical Properties of Raw Wastes</i>	56
3.2.2	<i>Trial Waste Mixes and their Properties</i>	58
3.3	TEST METHODOLOGY	59
3.3.1	<i>Modified Proctor Test</i>	59
3.3.2	<i>California Bearing Ratio</i>	59
3.3.3	<i>Unconfined Compressive Strength</i>	60
3.3.4	<i>Durability Test</i>	60
3.3.5	<i>Cyclic Load Triaxial Test</i>	61
3.4	RESULTS AND DISCUSSION	63
3.4.1	<i>Modified Proctor Test</i>	63

3.4.2	<i>Unconfined compressive strength</i>	64
3.4.3	<i>California Bearing Ratio</i>	68
3.4.4	<i>Durability characteristics</i>	69
3.4.5	<i>Triaxial Shear Strength</i>	69
3.4.6	<i>Resilient modulus</i>	72
3.5	SUMMARY	72
CHAPTER 4 DESIGN AND CONSTRUCTION OF TEST SECTIONS		75
4.1	INTRODUCTION	75
4.2	TEST LOCATION.....	75
4.3	DESIGN OF THE TEST SECTION	76
4.4	SUBGRADE STABILIZATION AND QUALITY CONTROL	78
4.4.1	<i>Natural Subgrade and stabilization using Flyash</i>	78
4.4.2	<i>Light Weight Deflectometer (LWD) Test</i>	80
4.4.3	<i>Dynamic Cone Penetrometer Test (DCPT)</i>	81
4.5	SUBBASE CONSTRUCTION AND QA/QC	82
4.5.1	<i>Mixing and Laying</i>	82
4.5.2	<i>Leachate collection System</i>	83
4.5.3	<i>Compaction</i>	83
4.5.4	<i>Curing</i>	83
4.5.5	<i>Quality control</i>	86
4.5.6	<i>DCPT and Field CBR</i>	88
4.5.7	<i>Light Weight Deflectometer test</i>	89
4.6	SUMMARY	90
CHAPTER 5 FIELD PERFORMANCE OF TEST SECTIONS		91
5.1	INTRODUCTION	91
5.2	POST CONSTRUCTION TEST PLAN.....	91

5.3	STRUCTURAL EVALUATION USING FWD	93
5.3.1	<i>Dynatest 8000 Falling Weight Deflectometer</i>	93
5.3.2	<i>FWD testing Technique.....</i>	94
5.3.3	<i>Corrections to FWD Deflections.....</i>	94
5.3.4	<i>Deflection based Parameters for structural evaluation</i>	95
5.3.5	<i>Backcalculation of falling weight deflectometer modulus (E_{FWD}).....</i>	97
5.3.6	<i>Statistical significance for comparison of structural performance</i>	100
5.4	CORING OPERATION AND MICROSTRUCTURE ANALYSIS	101
5.5	FUNCTIONAL PERFORMANCE USING BUMP INTEGRATOR.....	103
5.6	TRUCK OVERLOADING TEST	103
5.7	DETECTION OF HEAVY METAL CONTAMINATION.....	104
5.8	RESULT AND DISCUSSION	105
5.8.1	<i>Coring Operation</i>	105
5.8.2	<i>Traffic measured during study.....</i>	112
5.8.3	<i>Initial Structural performance using DBPs.....</i>	113
5.8.4	<i>Seasonal variation in structural performance.....</i>	119
5.8.5	<i>Summary of DBPs and Failure mechanism of test sections</i>	122
5.8.6	<i>Backcalculated Moduli of all layers.....</i>	124
5.8.7	<i>Backcalculated Moduli of Subbase layers.....</i>	126
5.8.8	<i>Functional performance of test sections.....</i>	130
5.8.9	<i>Leaching Tests.....</i>	132
5.8.10	<i>Remaining Service life ratio and maintenance requirements</i>	134
5.9	SUMMARY	136

CHAPTER 6 COMPARING LABORATORY & FIELD MODULI.....138

6.1	INTRODUCTION	138
6.2	METHODOLOGY	139
6.2.1	<i>Determination of the Field State of stress under multiload FWD tests.....</i>	140

6.3	RESULTS AND DISCUSSION	140
6.3.1	<i>Laboratory Resilient modulus.....</i>	140
6.3.2	<i>Structural evaluation of the test sections by FWD.....</i>	142
6.3.3	<i>Variation of backcalculated moduli of subbase layers with stress and curing.</i>	146
6.3.4	<i>Variation of deviatoric and confining stresses in subbase layer</i>	149
6.3.5	<i>Modelling the resilient modulus response in laboratory and field.....</i>	150
6.3.6	<i>Correlation between the M_r and E_{FWD}</i>	155
6.4	SUMMARY	159
CHAPTER 7 COMPARATIVE LIFE CYCLE AND COST ANALYSIS		161
7.1	INTRODUCTION	161
7.2	LCA METHODOLOGY	162
7.2.1	<i>Goal and Scope.....</i>	162
7.2.2	<i>System Boundary</i>	163
7.2.3	<i>Functional Unit.....</i>	163
7.2.4	<i>Life Cycle Inventory data and quality requirements.....</i>	164
7.2.5	<i>Allocation.....</i>	164
7.3	LIFE CYCLE INVENTORY DATABASE	165
7.3.1	<i>Natural aggregate.....</i>	165
7.3.2	<i>Granulated Blast Furnace Slag and Copper slag.....</i>	167
7.3.3	<i>Land Use.....</i>	169
7.3.4	<i>Mixing Operations and Construction activities.....</i>	169
7.3.5	<i>Transportation.....</i>	173
7.4	LIFE CYCLE IMPACT ASSESSMENT	173
7.5	RESULTS AND DISCUSSION	176
7.5.1	<i>LCIA of subbase materials.....</i>	176
7.5.2	<i>Comparative LCIA of test sections across the life cycle stages.....</i>	176
7.5.3	<i>Sensitivity of LCI to economic allocation.....</i>	184

7.5.4	<i>Uncertainty analysis</i>	186
7.5.5	<i>Life Cycle costs</i>	188
7.6	SUMMARY	189
CHAPTER 8 CONCLUSIONS		193
8.1	GENERAL	193
8.2	CONCLUSIONS	194
8.2.1	<i>Laboratory testing for Optimum mix</i>	194
8.2.2	<i>Construction of the test sections</i>	195
8.2.3	<i>Field Performance of the test sections</i>	195
8.2.4	<i>Comparison between laboratory and field moduli</i>	197
8.2.5	<i>Life cycle assessment and cost analysis</i>	198
8.3	FUTURE SCOPE	199
REFERENCES		201

LIST OF FIGURES

Figure 1.1 Flowchart showing details of field tests and laboratory experiments.	8
Figure 2.1 Copper Production Procedure (Vaccari and Tikana 2017).....	13
Figure 2.2 Copper smelting technologies and mass flow details	14
Figure 2.3 Layout of typical blast furnace process (Remus et al. 2013).....	17
Figure 2.4 Working principle of FWD (IRC 115, 2014)	19
Figure 2.5 Pavement structure of different test sections (Edil et al. 2002).....	22
Figure 2.6 Leachate collection system (Edil et al. 2002).....	22
Figure 2.7 Change in average volumetric water content (left) and maximum deflection under 90 kN (right) FWD load in different seasons (Edil et al. 2002)	23
Figure 2.8 LSME setup (left) and schematic experimental setup (right) (Tanyu et al. 2003) .	24
Figure 2.9 Details of the test tracks and layer properties (Tanyu et al. 2003)	25
Figure 2.10 Cost of construction for different test sections (Li et al. 2019).....	29
Figure 2.11 Composite modulus and layer modulus for different macadam section compared with CBR values measure by DCP tests after construction (Li et al. 2019).....	29
Figure 2.12 E_{FWD} / M_r against M_r (Nazzal and Mohammad 2010).....	33
Figure 2.13 Light weight deflectometer moduli compared with laboratory resilient moduli Nazzal and Mohammad 2010)	33
Figure 2.14 Pavement Elastic and visco-elastic behavior as evident from the deflection time history (left) and hysteresis loop (right) (Deblois et al. 2010).....	35
Figure 2.15 Comparison between hysteretic behaviour for seasons (left) and dissipated energy calculated at different offsets for seasons (right) (Deblois et al. 2010)	36
Figure 2.16 Instrumented pavement (Salour and Erlingsson 2012, 2013a; b).....	36
Figure 2.17 Subsurface Volumetric Moisture content in unbound layers and maximum deflections under 50 kN FWD loads (Salour and Erlingsson 2012, 2013a; b).....	37

Figure 2.18 Back calculated moduli of granular layer (a) and subgrade (b) and VMC (Salour and Erlingsson 2012, 2013a; b)	38
Figure 2.19 Seasonal variation in peak FWD Deflections (Norouzi et al. 2013).....	38
Figure 2.20 Relation between normalised BDI and DBDI with k_1 of aggregate base (Park et al. 2005).....	41
Figure 2.21 Deflection basin under HWD load and Modified BDI and BCI adopted (Donovan and Tutumluer 2009)	42
Figure 2.22 Pavement conditions of (a) FM 800 and (b) FM 1761; (c) FWD testing on FM 800; (d) visible cracks on top of lime-treated caliche base (Chen et al. 2011)	46
Figure 2.23 Distress at SH 24 (a) reflective crack and core location; (b) cracks on CTB layer (c) full depth core with cracks on HMA and CTB layers; (d) cracks in HMA and CTB layers (Chen et al. 2011).....	47
Figure 3.1 Test location and locations of the raw material sources used in the study	55
Figure 3.2 Raw wastes used in the study and the granular subbase material	56
Figure 3.3 Cyclic load triaxial (CTT) test setup used in this study (SVNIT Surat)	61
Figure 3.4 Haversine waveform for cyclic load test (AASHTO 2000).....	63
Figure 3.5 Modified Proctor compaction curves for different trial mixes	64
Figure 3.6 Change in UCS with curing period for a)FAL, b)FAG and c)CFA trial mixtures and flyash (Optimum mixes highlighted in box).....	66
Figure 3.7 UCS specimens of optimum fly ash-lime (FAL) and fly ash-GBFS (FAG) mixtures after failure	67
Figure 3.8 Comparison of deviator stresses at failure for optimum mixes of fly ash-lime (FAL), fly ash-GBFS (FAG) and GSB at various curing periods.....	70
Figure 3.9 Comparison of elastic modulus at failure for optimum mixes of fly ash-lime (FAL), fly ash-GBFS (FAG) and GSB at various curing periods	71
Figure 3.10 Grain size distribution of materials used in subbase	73

Figure 4.1 Location of test tracks (Google Earth Image) near Kadrama village on GJ-SH 6 .	75
Figure 4.2 Details of the test sections used in the study	77
Figure 4.3 Construction of stabilized subgrade and quality control testing.....	79
Figure 4.4 Test plan for all the field tests carried out on a typical test section.....	80
Figure 4.5 Average penetration against the number of hammer blows	82
Figure 4.6 Mixing procedures for CFA and FAG (batching plant and machine mixing).....	84
Figure 4.7 Construction of CFA (mixing at the plant, similar procedure for FAG).....	84
Figure 4.8 Construction of FAL (in-situ mixing)	85
Figure 4.9 Preparation of filed mix cylindrical samples at mixing plant.....	85
Figure 4.10 Pipe lying operation (SB 3, FAG 400)	85
Figure 4.11 Quality Control using a) DCPT, b) LWD, c) Field density, d) Field CBR on subbase layers	87
Figure 4.12 LWD modulus of FAL, FAG, CFA and GSB layers recorded at nine test locations within 50 m long test section after 7-days of construction.	89
Figure 5.1 Dynatest 8000 Falling Weight Deflectometer	93
Figure 5.2. Backcalculation algorithm and finite element model used in the study	97
Figure 5.3 Comparison between recorded and calculated deflection basins at different E_2/E_3	99
Figure 5.4 (a)Ultima IV XRD instrument, (b) powdered FAL sample.....	101
Figure. 5.5 (a) samples mounted on the disc, (b) samples after gold coating and (c) Zeiss's EVO 18 tabletop SEM	102
Figure 5.6 Photographs of coring operation.....	107
Figure 5.7 X-ray diffraction pattern of waste mixes cured for 270 days in lab and field Q - Q -Quartz (SiO_2), S -Calcium Sulfate Anhydrite (CaSO_4), C -Calcite (CaCO_3), A - Aluminum Oxide (Al_2O_3), E -Ettringite ($\text{Ca}_3\text{Al}_1(\text{SO}_4)_{1.5}(\text{OH})_6 \cdot 13\text{H}_2\text{O}$), G -Dicalcium AluminoSilicate ($\text{Al}_2\text{Ca}_2\text{SiO}_7$), F -Magnetite (Fe_3O_4). P -Magnesium Oxide (MgO)	109

Figure 5.8 SEM images of waste mix samples cured in lab (field mix) and field (cores) for 270 days.....	111
Figure 5.9 Peak deflection and area under pavement profile after 90 days of curing	114
Figure 5.10 Curvature Indices observed after 90 days of curing.....	115
Figure 5.11 Surface moduli values exhibited by the test sections after 90 days of curing.....	118
Figure 5.12 Relationship between normalized S_{300} and BDI for all waste mix test sections .	119
Figure 5.13 Hysteretic loops exhibited by different test sections under 40 kN FWD load after 60 days of curing and calculation of the dissipated energy.....	120
Figure 5.14 Initial, pre- and post-monsoon dissipated energy exhibited by test sections in two years.....	121
Figure 5.15 Temporal changes in DE in test sections with 300 mm thick subbase layers.....	122
Figure 5.16 Summary of median of deflection basin parameters recorded over complete project duration.....	123
Figure 5.17 Summary of change in backcalculated moduli of waste mixes and GSB due to curing, seasonal variation and truck loading	128
Figure 5.18 Side drain water levels (a) post-monsoon 2019, (b) pre-monsoon 2020	129
Figure 5.19 Summary of Unevenness Index using fifth wheel Bump Integrator.....	131
Figure 5.20 Rutting recorded on left lane of a) FAL 300 and b) Control section (GSB 330)	132
Figure 6.1. Flow chart of the methodology	139
Figure 6.2 Effect of deviator and confining stress on the resilient modulus of waste mixes cured for 7 days.	141
Figure 6.3 Effect of curing on the resilient modulus (at $\sigma_3 = 34.45$ kPa and $\sigma_d = 103.35$ kPa) of waste mixes	142
Figure 6.4 Effect of FWD load on Peak deflection response of test sections	143
Figure 6.5 Hysteresis loop of load -deflection history observed on CFA 400 under multiload level FWD tests normalised for 40 kN load	144

Figure 6.6 Comparison between plots of surface moduli of CFA 400 and FAG 400 test sections under 40 kN and 70 kN FWD loads in Oct 2018.....	146
Figure 6.7 Variation in subbase E_{FWD} with curing period and traffic loading in (a) FAL 400, (b) FAG 400 and (c) CFA 400 layers.	148
Figure 6.8 Effect of subbase thickness on the backcalculated FWD modulus and average bulk stress under 40 kN load after 60 days of curing.....	149
Figure 6.9 Summary of mean deviator and confining stresses calculated in 300 mm thick waste mix subbase layers under 40 kN (standard axle load)	150
Figure 6.10 Recorded and Predicted subbase E_{FWD} used for (A) training and (B) testing the bulk stress model of FAL subbases after 30 days of curing	152
Figure 6.11 Implementation of stress-dependent conversion factors to evaluate design subbase modulus.....	159
Figure 7.1 Steps in Life Cycle Assessment.....	161
Figure 7.2 System boundary adopted for the analysis of the test sections.....	163
Figure 7.3 Relations between impact categories at midpoint and endpoint in ReCiPe 2016	174
Figure 7.4 Stage wise relative life cycle impacts of waste mix test sections as a percent of control section.....	179
Figure 7.5 Stage wise relative life cycle impacts for control section	180
Figure 7.6 Relative life cycle impacts at endpoint impact categories for all the test sections compared to control	181
Figure 7.7 Effect of economic allocation on the life cycle impacts of waste mix and control test sections of same thickness.....	185
Figure 7.8 Results of Monte Carlo uncertainty analysis for control vs waste mix sections for no and economic allocation	187

LIST OF TABLES

Table 2.1 Mass flow balance in pig iron production	16
Table 2.2 Evaluated from the plate load test corresponding to 1.5 mm deflection (Kumar and Kumar 2000).....	21
Table 2.3 Geotechnical characterization and strength of subbase materials (Edil et al. 2002)	21
Table 2.4 Properties of granular materials (Tanyu et al. 2003).....	24
Table 2.5 Moduli of granular materials based on CTT, FWD, LSME (Tanyu et al. 2003)	24
Table 2.6 Elastic modulus and CBR of the optimum waste mix and conventional materials (Bin-Shafique et al. 2004)	26
Table 2.7 Mix designations adopted for various mix proportions (Havanagi et al. 2007, 2008)	28
Table 2.8 UCS test results of trial mixes (Havanagi et al. 2007, 2008)	28
Table 2.9 Summary of field studies	30
Table 2.10 Summary of studies o correlating E_{FWD} lab M_r	34
Table 2.11 Summary of seasonal variation in pavements monitored using FWD	39
Table 2.12 Equation for different critical pavement responses derived using DBPs (Park and Kim 2003).....	40
Table 2.13 Summary of applications of DBPs	43
Table 2.14 Comparison of 20-year traffic, base layer characteristic and field performance (Chen et al. 2011)	47
Table 3.1 Unit rates and source of materials	56
Table 3.2 Physical properties of waste materials	57
Table 3.3 Chemical Composition of raw waste materials in percentage by weight.....	57
Table 3.4 Loading sequences used in cyclic load triaxial testing as per AASHTO T307 (AASHTO 2000)	62

Table 3.5 Soaked CBR values of different fly ash-lime and fly ash-GBFS mixes.....	69
Table 3.6 Shear strength parameters of FAL, FAG and CFA with curing periods	72
Table 3.7 Optimum industrial waste mix with their strength and stiffness parameters.....	74
Table 4.1 Properties of subgrade soil.....	78
Table 4.2 Results of LWD and DCPT tests conducted on the stabilized subgrade	81
Table 4.3 Field Density details (FDD – field dry density).....	86
Table 4.4 Results of LWD, DCPT and field CBR tests conducted on FAG and CFA subbase	88
Table 4.5 Correlations between PI and Field CBR.....	88
Table 5.1 Summary of the FWD tests and the phases of the field study	92
Table 5.2. Deflection basin parameters used in the study.....	96
Table 5.3. Target design and actual constructed thickness of different pavement layers (for schematic diagram of the layers, please refer to Fig. 4.2)	105
Table 5.4 UCS, M_r , E_{sb} and E_{sb}/M_r of field cores samples (CORE), two laboratory-cured field samples (LAB-FLD) and laboratory mix samples (LAB) of FAL, FAG and CFA.	106
Table 5.5. X-Ray diffraction peak count (in percentage) of the raw flyash and the waste mix samples cured for 270 days in lab and in the field.....	110
Table 5.6 Summary of traffic volume experienced by the test sections	112
Table 5.7 Result of the Games Howell test presented in terms of the probability values (similar trend after 2 years).....	116
Table 5.8 Pavement condition threshold values of peak deflection and curvature indices corresponding to 40 kN contact stress.	117
Table 5.9 Summary of the evolution of E_{FWD} (MPa) with curing period under 40 kN target load of all layers of test sections	125
Table 5.10 TCLP test results (all concentrations in mg/l)	133

Table 5.11 Single batch water leaching test results.....	134
Table 5.12 Heavy metal concentrations in drain lachate (all concentrations in mg/l)	134
Table 5.13 Summary of the 85 th percentile E _{FWD} of different layers at initial, 2 year and end of test period	135
Table 5.14 Remaining service life ratio of test sections at initial, 2 year and end of test period and overlay thickness (BC and DBM) required at the end of test period.....	136
Table 6.1. Model constants for waste mix in laboratory and field at different curing periods	153
Table 6.2 Stress-dependent conversion coefficients for waste mixes and SLR for test sections with 300 mm thick subbase	157
Table 7.1 Direct burdens of producing one ton of natural aggregates	166
Table 7.2 Details of land use and occupation in production of Natural aggregate.....	167
Table 7.3 Details of economic allocation used in the study	168
Table 7.4 Energy and emissions during granulation and dumping of raw wastes	170
Table 7.5 Energy required from burning diesel fuel in different construction equipments. ...	171
Table 7.6 Details of unit processes, functional units, type and source of LCI data	172
Table 7.7 Overview of midpoint Impact categories as per ReCiPe 2016.....	175
Table 7.8 Life cycle impacts per m ³ of waste mixes compared with GSB*	178
Table 7.9 Life cycle impacts* of as-constructed waste mixes compared with control section#	182
Table 7.10 Details of the overall cost of construction.....	189
Table 7.11 Test sections - design parameters, construction cost and service life ratio, overlay requirement and Relative Life cycle impact score at endpoint	190

LIST OF ABBREVIATIONS

AASHTO	American Association of State Highway and Transportation Officials
ASTM	American Society for Testing and Materials
AUPP	Area Under Pavement Profile
BC	Bituminous Concrete
BCI	Base Damage Index
BDI	Base Curvature Index
BDL	Below Detection Limit
BF	Blast Furnace
BFS	Blast Furnace Slag
BI	Bump Integrator
BS	British Standards
CF	Conversion Factors
CFA	Copper slag (70%) + Fly Ash (30%) mix
CASH	Calcium Alumino-Silicate Hydrate
CBR	California Bearing Ratio
CSH	Calcium Silicate Hydrate
CoV	Coefficient of Variance
CRRI	Central Road Research Institute
CS	Copper Slag
CTB	Cement Treated Base
CTT	Cyclic Triaxial Test
CVPD	Commercial Vehicles Per Day
DCPT	Dynamic Cone Penetrometer Test
DBM	Dense Bituminous Macadam
DBP	Deflection Basin Parameters
DE	Dissipated Energy
DoI	Depth of Influence
DST	Department of Science and Technology
ECD	European Council Decision
EPD	Electronic Product Declarations
ESAL	Equivalent Standard Axle Load

EU	European Union
FA	Fly Ash
FAG	80% FlyAsh + 20% Granulated blast furnace slag
FAL	Flyash + 5% Lime
FD	Fossil fuel Depletion
FE	Freshwater Eutrophication
FEM	Finite Element Method
FHWA	Federal Highway Administration
Ftox	Freshwater ecotoxicity
FWD	Falling Weight Deflectometer
GBFS	Granulated Blast Furnace Slag
GoI	Government of India
GSB	Granular Sub Base
GW	Well graded Gravel
GWP	Global Warming Potential
HCtox	Human Carcinogenic toxicity
HMA	Hot Mix Asphalt
HNCtox	Human Non-Carcinogenic toxicity
IIT	Indian Institute of Technology
INR	Indian National Rupee
IQR	Inter-Quantile Region
IR	Ionizing Radiation
IRC	Indian Roads Congress
IRI	International Roughness Index
IS	Indian Standards
ISO	International Organization for Standardization
kN	Kilo Newton
kPa	Kilo Pascal
LCA	Life Cycle Assessment
LCCA	Life Cycle Cost Assessment
LCI	Life Cycle Inventory
LCIA	Life Cycle Impact Assessment
LCV	Light Commercial Vehicle
LO	Land Use

LPH	Liters Per Hour
LPT	Litres Per Ton
LWD	Light Weight Deflectometer
MD	Mineral resource Scarcity
MDD	Maximum Dry Density
ME	Marine Eutrophication
ML	Low Compressible Silt
MoRTH	Ministry of Road Transport and Highways
MPa	Mega pascal
msa	million standard axles
MT	Mega Ton
Mtox	Marine ecotoxicity
NCHRP	National Cooperative Highway Research Program
ND	Not Detected
NL	No Limit
NT	Not Tested
OD	Ozone Depletion
OFH	photochemical Oxidant Formation: Human health
OMC	Optimum Moisture Content
OFT	photochemical Oxidant Formation: Terrestrial ecosystem
PI	Penetration Index
PL	Plastic limit
PLT	Post Truck over Loading
PM	Particulate Matter
PMF	Particulate Matter Formation
RA	Terrestrial Acidification
RAP	Reclaimed Asphalt Pavement
RMS	Root Mean Square
SC	Stress Combination
SCI	Surface Curvature Index
SD	Standard Deviation
SEM	Scanning Electron Microscopy
SH	State Highway
SLR	Service Life Ratio

SM	Silty Sand
SN	Structural number
SP	Poorly graded sand
SVNIT	Sardar Vallabhbhai National Institute of Technology
SW	Well-graded Sand
TCLP	Toxicity characteristic leaching procedure
Ttox	Terrestrial ecotoxicity
UCS	Unconfined compressive strength
UI	Unevenness Index
USD	United States Dollar
US EPA	United States Environmental Protection Agency
UU	Unconsolidated Undrained
VDF	Vehicle Damage Factor
VMC	Volumetric Water Content
WC	Water Consumption
WMM	Wet Mix Macadam
XRD	X-Ray Diffraction

LIST OF NOTATIONS

ϕ	Angle of internal friction
θ	Bulk stress
ν	Poisson's ratio of sand
$^{\circ}\text{C}$	Degree Celsius
δ	Maximum deformation on the pavement surface
ϵ_r	Elastic axial strain
ϵ_t	Elastic horizontal tensile strain
ϵ_v	Elastic vertical compressive strain
σ_3	Confining pressure
σ_d	Deviator stress
σ_1	Major principal stress
σ_{cyclic}	repeated axial stress
τ	Maximum shear stress
τ_{oct}	Octahedral Shear Stress
a	diameter of the loading plate
a, b, c, d and e	conversion coefficients defining conversion factors
Al	Aluminum
Al_2O_3	Aluminum oxide
As	Arsenic
Ba	Barium
c	Cohesion intercept
CaCO_3	Calcite
CaO	Calcium oxide (Lime)
CaSO_4	Calcium Sulphate Anhydrite
$\text{Ca}_2\text{Al}_2\text{SiO}_7$	Dicalcium AluminoSilicate
$\text{Ca}_3\text{Al}_1(\text{SO}_4)_{1.5}(\text{OH})_6 \cdot 13\text{H}_2\text{O}$	Ettringite
Cc	Compression index
Cd	Cadmium
Co	Cobalt
Cr	Chromium

Cu	Copper
D_0	Peak deflection under FWD load
$D_{300 \text{ to } 1800}$	Peak deflection at radial distances 300 mm to 1800 mm
E	Secant modulus of elasticity
$E_{1 \text{ to } 4}$	Backcalculated field moduli of HMA, WMM, subbase and subgrade
E_{FWD}	Backcalculated field modulus using FWD
E_{LWD}	Backcalculated field modulus using LWD
E_{sb}	Backcalculated subbase layer modulus
Fe	Iron
Fe_2O_4	Magnetite
k	Permeability
k_0	Coefficient of lateral earth pressure at rest
k_1, k_2	regression coefficients for bulk stress model
k_3, k_4, k_5	regression coefficients for NCHRP model
L/S	Liquid to Solid ratio
MgO	Magnesium oxide
Mn	Manganese
MnO	Manganese oxide
Mo	Molybdenum
M_r	Resilient modulus (laboratory)
Ni	Nickel
p	probability
P_a	Atmospheric pressure
Pb	Lead
q_u	Unconfined compressive strength
R_i	Resistance Index
R^2	Coefficient of determination
$S_0 - S_{1800}$	Surface moduli at radial distance 0 to 1800 mm
SiO_2	Silicon dioxide
SO_4	Sulphates
Zn	Zinc